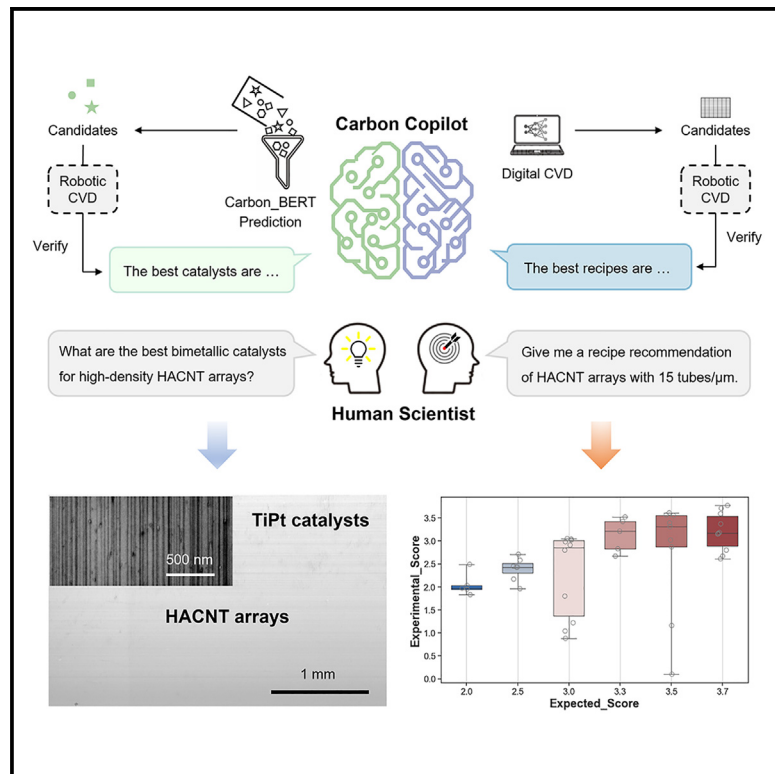


# Transforming the synthesis of carbon nanotubes with machine learning models and automation

## Graphical abstract



## Authors

Yue Li, Shurui Wang, Zhou Lv, ...,  
Yaodong Yang, Ziqiang Zhao, Jin Zhang

## Correspondence

qianliu-cnc@pku.edu.cn (L.Q.),  
yaodong.yang@pku.edu.cn (Y.Y.),  
zqzhao@pku.edu.cn (Z.Z.),  
jinzhang@pku.edu.cn (J.Z.)

## In brief

This study presents an AI-driven platform, Carbon Copilot (CARCO), that transforms the research paradigm of carbon-based nanomaterials. CARCO integrates machine learning and automation to overcome key challenges in carbon nanotube production, including catalyst innovation and precise growth control. This approach significantly accelerates the research process and highlights the potential of AI to reshape materials science.

## Highlights

- AI-driven platform for carbon nanotube synthesis
- AI-recommended TiPt catalyst outperforms traditional Fe catalysts
- Achieved high-accuracy density control in HACNT arrays synthesis

## Improvement

Enhanced performance with innovative design or material control



Li et al., 2025, Matter 8, 101913  
January 8, 2025 © 2024 Published by Elsevier Inc.  
<https://doi.org/10.1016/j.matt.2024.11.007>



## Article

# Transforming the synthesis of carbon nanotubes with machine learning models and automation

Yue Li,<sup>1,2,5</sup> Shurui Wang,<sup>1,3,5</sup> Zhou Lv,<sup>1</sup> Zhaoji Wang,<sup>4</sup> Yunbiao Zhao,<sup>2</sup> Ying Xie,<sup>1</sup> Yang Xu,<sup>2</sup> Liu Qian,<sup>1,\*</sup> Yaodong Yang,<sup>4,\*</sup> Ziqiang Zhao,<sup>1,2,\*</sup> and Jin Zhang<sup>1,3,6,\*</sup>

<sup>1</sup>School of Materials Science and Engineering, Peking University, Beijing 100871, China

<sup>2</sup>State Key Laboratory of Nuclear Physics and Technology, School of Physics, Peking University, Beijing 100871, China

<sup>3</sup>Beijing Science and Engineering Center for Nanocarbons, Beijing National Laboratory for Molecular Sciences, College of Chemistry and Molecular Engineering, Peking University, Beijing 100871, China

<sup>4</sup>Institute for AI, Peking University, Beijing 100871, China

<sup>5</sup>These authors contributed equally

<sup>6</sup>Lead contact

\*Correspondence: [qianliu-cnc@pku.edu.cn](mailto:qianliu-cnc@pku.edu.cn) (L.Q.), [yaodong.yang@pku.edu.cn](mailto:yaodong.yang@pku.edu.cn) (Y.Y.), [zqzhao@pku.edu.cn](mailto:zqzhao@pku.edu.cn) (Z.Z.), [jinzhang@pku.edu.cn](mailto:jinzhang@pku.edu.cn) (J.Z.)  
<https://doi.org/10.1016/j.matt.2024.11.007>

**PROGRESS AND POTENTIAL** Carbon-based nanomaterials (CBNs) have revolutionized materials science with their outstanding properties but face bottlenecks in synthesis that fail to meet application demands. As research interest has transitioned from small demos in labs to industrial applications, challenges such as reproducibility, uniformity, and the statistical significance of indicators have magnified, making traditional methods inadequate. Overcoming these challenges requires new research paradigms. AI technology, which excels in exploring complex scientific systems, offers new pathways to address these long-standing challenges. In response, we developed an AI-driven platform tailored for CBNs named Carbon Copilot (CARCO). We applied CARCO to the highly promising yet challenging domain of horizontally aligned carbon nanotube (HACNT) arrays and addressed two significant challenges. First, through high-throughput screening, CARCO identified a groundbreaking titanium-platinum bimetallic catalyst, outperforming the traditional iron catalyst, known since the 2000s as optimal for growing high-density HACNT arrays. Additionally, CARCO enabled density-controllable growth through the assistance of virtual experiments, greatly enhancing customization for various applications. Notably, these achievements were accomplished within just 43 days, a time frame significantly shorter than the traditional research process, which could extend over a year.

## SUMMARY

Carbon-based nanomaterials (CBNs) hold immense promise in electronics, energy, and mechanics. However, their practical applications face synthesis challenges stemming from complexities in structural control, large-area uniformity, and consistency, unaddressed by current research methodologies. Here, we introduce carbon copilot (CARCO), an artificial intelligence (AI)-driven platform that integrates transformer-based language models, robotic chemical vapor deposition (CVD), and data-driven machine learning models. Employing CARCO, we discovered a novel titanium-platinum bimetallic catalyst for high-density horizontally aligned carbon nanotube (HACNT) array synthesis, outperforming traditional catalysts. Furthermore, leveraging millions of virtual experiments, we achieved an unprecedented 56.25% precision in synthesizing predetermined densities of HACNT arrays. All were accomplished within just 43 days. This work not only advances the field of CBNs but also exemplifies the integration of AI with human expertise to overcome the limitations of traditional experimental approaches, marking a paradigm shift in nanomaterials research and paving the way for broader applications.

## INTRODUCTION

Carbon-based nanomaterials (CBNs), such as carbon nanotubes (CNTs) and graphene, have revolutionized materials sci-

ence with their exceptional electrical, mechanical, and thermal properties.<sup>1,2</sup> From facilitating the fabrication of electronics that surpass the limits of Moore's Law,<sup>3</sup> to upgrading the performance of lightweight and high-strength structural materials,<sup>4</sup> to

enhancing the efficiency of energy storage,<sup>5</sup> CBNs have embarked on a significant journey in advanced materials. However, the full potential of CBNs is often hindered by challenges in synthesizing products with controllable structures, large-area uniformity, and high yield, which are critical for their transition from laboratory research to industrial applications.

This conundrum is a microcosm of the intrinsic challenges prevalent in the development of nanomaterials. Essentially, the journey from atomic assembly to wafer-scale production spans numerous dimensions, exposing the limitations of traditional research methodologies when confronted with such complex systems. Within the conventional scientific paradigm, innovation is often driven by hypothesis-deductive reasoning or analogical reasoning. Hypothesis-deductive reasoning, while powerful in simpler systems, struggles to capture the multi-variable and multi-layered interactions inherent in complex systems like CBN synthesis. Analogical reasoning, which identifies similar modes and relationships across different systems, is applicable even in high-dimensional complexities and has been widely employed in the development of nanomaterials. However, the success of analogical reasoning heavily depends on extensive expertise, and transferring analogies becomes harder when a field evolves, hindering further breakthroughs.

Once a feasible innovative method for CBN synthesis is identified, the research focus shifts to optimizing the experimental process and analyzing the outcomes. This phase unveils another challenge: the complex chemical interactions during the synthesis process, involving poorly understood mechanisms, often lead to difficulties in interpreting the relationship between synthesis recipes and sample performance. Nevertheless, traditional academic optimization and analyzing strategies, which primarily rely on the “one-factor-at-a-time” (OFAT) method, are inadequate in addressing the coupling effects of various synthesis variables such as catalysts, temperature, and growth substrates, resulting in misunderstandings of the growth mechanisms and overlooking of global optimum conditions.<sup>6</sup>

In response to these challenges, there is a pressing need to transform the research paradigm for CBN synthesis. Machine learning (ML) methods, known for their proficiency in navigating the complexities of nonlinear, highly coupled systems, have emerged as pivotal in this transformation.<sup>7</sup> Together with automation, they herald a new paradigm in scientific research. Recent advancements in materials synthesis, propelled by ML and automated experiments, are indeed exhilarating.<sup>8</sup> These advancements spanned diverse areas, including the prediction and synthesis of high-entropy alloys through literature mining,<sup>9</sup> the fabrication of nanoparticles by optimization algorithm,<sup>10–12</sup> and notably, the recent emergence of an artificial intelligence (AI)-agent platform for multiple chemical synthesis.<sup>13</sup> The application of this novel scientific paradigm holds tremendous potential in the realm of CBNs.

Therefore, we introduce an AI-driven autonomous chemical vapor deposition (CVD) platform called carbon copilot (CARCO) for the synthesis of CBNs. This platform integrates transformer-based language models, Carbon\_GPT and Carbon\_BERT, tailored for carbon nanomaterials based on GPTs and BERT, driving innovation in experimental design. Additionally, several data-driven ML models are designed to produce specific advice in the synthesis

process. Complementing these ML models is an automated CVD system, which acts as the “physical extension” of CARCO, enabling around-the-clock experiments and significantly boosting the efficiency and stability of CBN production.

As a demonstration of the effectiveness of CARCO, our research focused on the synthesis of horizontally aligned CNT (HACNT) arrays, which are regarded as pivotal materials for advancing next-generation electronics but encounter bottlenecks in precise synthesis.<sup>14</sup> Over a period of 43 days, CARCO exhibited marked advances in both catalyst innovation and controllable growth of HACNT arrays. Utilizing both Carbon\_GPT and Carbon\_BERT, we discerned a titanium-platinum (TiPt) bimetallic catalyst as a superior and groundbreaking alternative to conventional iron-based catalysts in CNT synthesis. Moreover, we achieved precision in synthesizing HACNT arrays at predetermined densities, marking a significant milestone considering the intricate variables involved. These achievements not only advance CNT development but also robustly validate the role of CARCO in the evolution of CBN research.

## RESULTS

### CARCO platform

The CARCO platform is structured around three interdependent core components: transformer-based language models,<sup>15</sup> robotic CVD, and data-driven ML models (Figure 1). Its modular design enables comprehensive coverage of the CBN fabrication research process while maintaining flexibility. Human scientists can design workflows targeting specific scientific questions, utilizing various modules as needed.

The transformer-based language models comprise Carbon\_GPT and Carbon\_BERT. Specifically, Carbon\_GPT was created based on OpenAI’s custom GPTs.<sup>16</sup> It is constructed by setting specific instructions and uploading a comprehensive knowledge base related to CBNs. This process tailors Carbon\_GPT to be adept at identifying and addressing scientific queries associated with carbon materials, thereby offering macro-scale academic insights. On the other hand, Carbon\_BERT was produced by fine-tuning BERT with a rich corpus of carbon-material-related literature. Carbon\_BERT excels in filtering tasks by utilizing word embedding techniques, such as selecting catalysts for CNT growth.<sup>17,18</sup>

The robotic CVD system encompasses several key parts: the CVD central controller, a mini-CVD, a robotic arm, an automated sample holder, and the sample stage (for more details, see Figure S1 and Video S1). The CVD central controller, designed using a programmable logic controller (PLC), executes unified command over the other hardware modules based on experimental parameters ordered by AI or human planners. The system features precise mechanical components for accurate sample placement and retrieval, coupled with meticulous regulation of temperature and gas phases, all situated within a cleanroom environment that maintains constant temperature and humidity levels. This system demonstrates a significant improvement in enhancing the efficiency and consistency of CVD experiments (Figure S2).

For typical synthesis research of CBNs, the robotic CVD system can conduct more than 30 reliable experiments daily. By

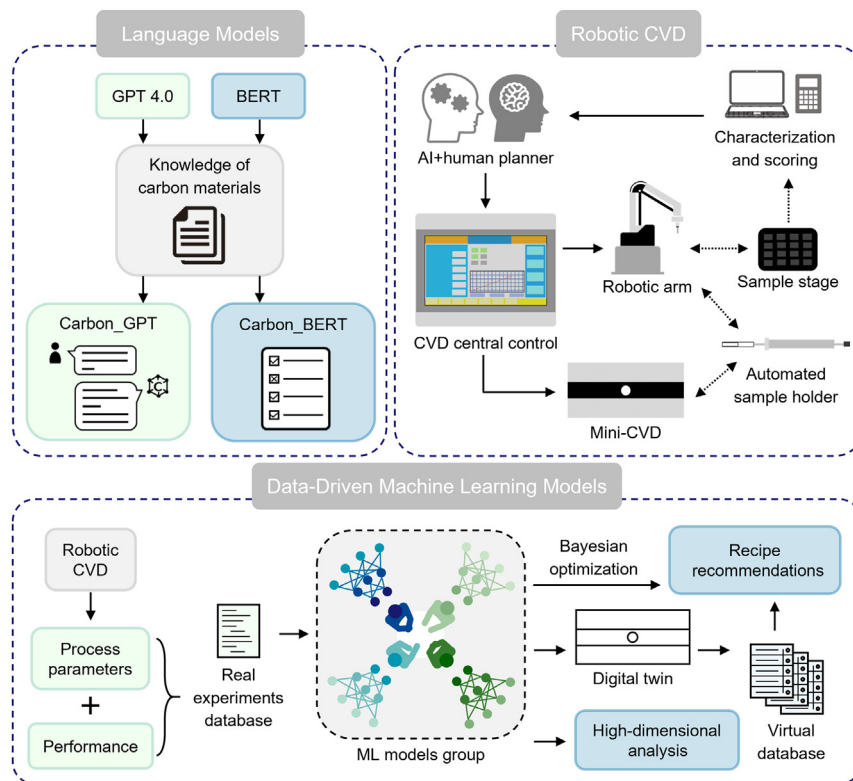


**Figure 1. Construction of CARCO platform**

The CARCO platform is composed of three modules: the language model module includes two transformer-based models customized with knowledge of carbon materials, Carbon\_GPT for question and answering (Q&A) tasks, and Carbon\_BERT for filtering tasks. The robotic CVD module is **orchestrated** by the CVD central control; solid arrows indicate the command flow, and dashed arrows show sample transfer. The data-driven machine learning (ML) model module centers around an ML model group built on a database, facilitating process recommendations and high-dimensional analysis tasks.

### Catalyst prediction and high-throughput screening

As the **inaugural** test of the CARCO platform, we embarked on an endeavor to identify innovative methods for the growth of high-density HACNT arrays. Leveraging the advanced capabilities of Carbon\_GPT, we explored potential strategies to enhance the density of HACNT arrays. Carbon\_GPT's analysis directed us toward several avenues: the optimization of growth conditions, use of tailored catalysts, substrate engineering, and the advance of controlled growth technologies (Figure S5). Among these, use of tailored cata-

collecting growth parameters and sample performance analyzed from characterization (Figure S3), it is possible to establish a standardized database **comprising** over 500 datasets within approximately 1 month. Leveraging such a high-quality database, we constructed a series of data-driven ML models. These models **adeptly** map the intricate relationships between CVD parameters and the resulting sample performance. In fact, a real-world CVD furnace essentially functions as a predictive model, where a specific set of parameters leads to a distinct performance outcome (Note S1). Considering the complexity of the parameter space for CBN synthesis, manually decoding these functional relationships through real-world CVD experiments is highly labor intensive. Hence, through our data-driven ML approach, we have developed a **digital twin** of the CVD process, which allows for the simulation of millions of experimental datasets within 20 min (Note S1), identifying appropriate growth parameters by exhaustive search or integrating strategies such as Bayesian optimization (BO) (Figure S4).<sup>19</sup> Additionally, these models provide crucial support in unraveling and analyzing the complex interactions between various process parameters and the resultant sample properties.

Emphasizing a collaborative approach, this platform integrates the strengths of AI and human scientists to explore and address intricate scientific challenges in CBN synthesis. Given that our automated system supports all CVD-based material systems and that the base model tailor approach is highly flexible, coupled with the universality of the data-driven ML method workflow, this platform also holds foreseeable potential in advancing a variety of other nanomaterials.

lysts, a relatively under-researched area recommended by Carbon\_GPT, caught our attention. Historically, iron-based catalysts have been favored for high-density HACNT array growth since the early 2000s.<sup>20</sup> The choice of catalysts, while intuitively linked to the structural control of CNTs,<sup>21</sup> bears a more complex relationship with array density. Factors like catalyst decomposition capability, carbon solubility, and behavior on substrates contribute to this complexity,<sup>22</sup> limiting the scope of exploration in this area for human scientists.

Addressing this multifaceted challenge, we employed a primarily screening approach of catalysts with a transformer-based language model, analyzing word embeddings for predictive insights. This method of leveraging word embeddings has already demonstrated significant potential in fields such as thermoelectric material prediction and precursor prediction of inorganic synthesis.<sup>23,24</sup> Rather than building a model from scratch, we utilized the open-source BERT model, fine-tuning it with carbon-material-specific literature, thus creating Carbon\_BERT. The training process and results are depicted in Figures 2A and S6. Carbon\_BERT analyzed the relationships between various catalysts and the concept of "high density" in HACNT arrays by transforming texts into word embeddings (Figure 2B). We ranked potential catalysts based on the cosine similarity between their embeddings and that of high density, predicting the likelihood of their efficacy in enhancing the density of HACNT arrays (Figures 2C, S6, and S7). This ranking was not only informed by the specialized knowledge embedded in Carbon\_BERT but was also enriched by the diverse insights inherited from BERT's extensive training on a wide range of topics. This method's

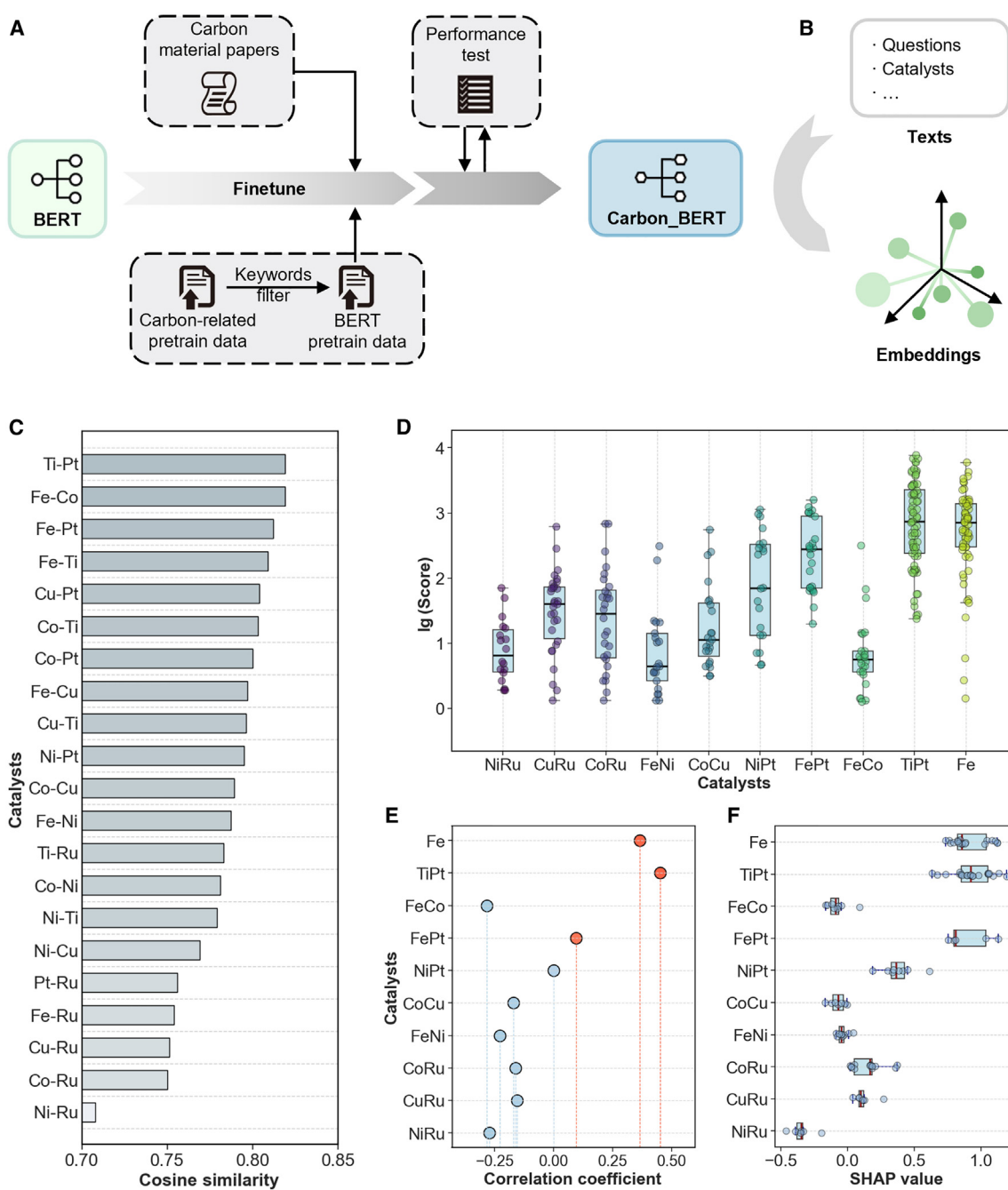


**Figure 2. Catalyst prediction and screening**

(A) Carbon\_BERT's fine-tuning process.

(B) Schematic representation from texts to embeddings.

(C) Rankings of cosine similarity for various bimetallic catalysts as derived from Carbon\_BERT.

(D) Density statistics of HACNT arrays with different catalysts.

(E) and (F) Spearman correlation coefficients and SHAP values for each catalyst, demonstrating their importance in the synthesis of high-density HACNT arrays, with TiPt showing superior performance over other combinations.

advantage lies in its ability to tap into the latent knowledge present in the language model, providing innovative suggestions that may not be immediately apparent through conventional scientific exploration.

The predictions regarding single-metal catalysts for CNT synthesis were consistent with the findings of experimental researchers according to previous reports.<sup>20,25</sup> However, due to the **scarcity** of literature on dual-metal catalysts, a direct

evaluation of these predictions was not feasible. Thus, we resorted to high-throughput automated experimentation for both validation and further screening. We selected nine catalyst combinations (three each from the top, middle, and bottom tiers of the prediction list) from the dual-metal predictions, along with conventional Fe as a control. These were loaded onto sapphire substrates using ion implantation technology, followed by the synthesis of HACNT arrays using the automated CVD platform. To ensure a fair comparison among different catalysts, a standardized parameter list was established (for more information, see Note S2 and Table S1). This list included 10 parameter sets that consistently led to favorable synthesis outcomes based on preliminary trials conducted by human scientists using a traditional Fe catalyst. Each catalyst underwent trials with all parameters in this list to establish a consistent baseline for subsequent experiments, and the order of sample growth was randomized to minimize any systematic bias. After that, each catalyst was further optimized manually or using BO, balancing consistency with adaptability. The samples were then characterized using scanning electron microscopy (SEM) and rated based on the density and orientation of the HACNT arrays. Analysis of the resulting database led to exciting findings, as depicted in Figures 2D and S8. The performance of most catalysts closely followed the order predicted by Carbon\_BERT except for FeCo. Notably, TiPt, ranked first by Carbon\_BERT and beyond conventional scientific expectations in the field of CNT growth, outperformed the traditional Fe catalyst in our experimental results (for more discussion, see Note S3).

To further mitigate the influence of catalysts on density performance, the database was analyzed employing both traditional statistical methods and ML techniques. Catalysts were encoded using the one-hot encoder, and Spearman's rank correlation coefficient analysis was utilized (Figure 2E). *p* values for all variables were found to be below 0.05, with the ranking of correlation coefficients displaying high consistency with the average sample performance obtained from experimental observations. Spearman's rank correlation coefficient offers a unidimensional correlation assessment between variables characterized by strong interpretability. However, it may not fully capture the complexities inherent in the relationships between variables. Consequently, encoded catalysts, in conjunction with the growth process and performance, were combined to develop a random forest regression (RFR) model, upon which the SHAP (Shapley additive explanations) method was applied to assess the importance of features for each catalyst (Figure 2F).<sup>26</sup> The RFR model, adept at processing high-dimensional data and complex feature interactions, in conjunction with SHAP, provides a quantifiable insight into each feature's predictive contribution. The outcomes were largely in agreement with the model's predictive ranking, suggesting that bias toward any specific catalyst was avoided in the experimental parameter settings. Such findings affirm the potential for catalyst prediction innovation through these AI methodologies. The effects of other variables on growth outcomes were also analyzed using these methodologies (Figure S9).

Investigating why TiPt is particularly suitable for the fabrication of high-density HACNT arrays necessitated a collaborative effort between human scientists and CARCO. Pt is known to be a good

catalyst, and our experiments also highlighted TiPt, FePt, and NiPt as standout formulations in the SHAP ranking. However, standalone Pt catalysts failed to produce uniformly distributed HACNT arrays. Specifically, Figure 3A shows SEM images of HACNT arrays synthesized using TiPt catalysts, demonstrating excellent uniformity at both millimeter and sub-millimeter scales. The inset in the top image shows a high-magnification SEM image, illustrating the high density and alignment of CNTs. Figure 3B shows typical SEM images of HACNT arrays synthesized using pure Pt catalysts. Compared to TiPt, the results from the Pt-only catalyst are highly non-uniform at the millimeter scale, with the HACNT arrays growing in clusters. Upon magnification, these clusters reveal regions with locally similar structures to those grown using TiPt. This comparison suggests that Pt is the primary catalyst for CNT growth, while Ti might play a role related to the support of Pt.

A thorough literature review revealed that the combination of Pt and TiO<sub>2</sub> is a common catalyst in the field of photoelectrocatalysis.<sup>27</sup> TiO<sub>2</sub> serves as an excellent carrier for Pt, and together, they form an ideal metal-semiconductor interface, exhibiting enhanced catalytic activity in hydrogen evolution reactions. To investigate whether a similar support behavior occurs in the TiPt system used for CNT growth, we further characterized the catalyst. Atomic force microscopy (AFM) analysis of a TiPt catalyst linked to a CNT (Figures 3C and 3D) revealed a layered structure suggestive of a support role: a lower layer, approximately 1.7 nm thick, likely representing a Ti-based oxide, and an upper nanoparticle layer of approximately 3.8 nm directly connected to the CNT, possibly representing Pt nanoparticles. Further X-ray photoelectron spectroscopy (XPS) analysis (Figure 3E) confirmed the only existence of Ti<sup>4+</sup>, suggesting that Ti is present as TiO<sub>2</sub>. This indicates that TiO<sub>2</sub> in the CNT growth system may play a role similar to that in photoelectrocatalysis, supporting the Pt and synergistically promoting the growth of high-density HACNT arrays.

Moreover, SEM characterizations of samples with Pt and TiPt catalysts (Figures S8, 3A, and 3B) showed that the resulting HACNT arrays were cleaner, with fewer bent tubes, and exhibited less carbon residuals. High-resolution transmission electron microscopy (HRTEM) (Figure 3F) and Raman spectra (Figure 3G) of the TiPt-grown samples confirmed the presence of single-walled CNTs (the diameter of a CNT is ~1.3 nm) with minimal defects, as indicated by the absence of a D-band. This may be related to complete carbon source decomposition of Pt. Detailed studies are currently underway to further investigate these phenomena, and the findings will be shared in future publications. Interestingly, Carbon\_GPT provided mechanistic insights that aligned well with those proposed by human scientists (Figure S10).

### Density-controllable synthesis

Having demonstrated the system's innovation in catalyst prediction and high-throughput screening, another intriguing question for us was its capability to achieve precise synthesis. HACNT arrays hold extensive potential in fundamental property research and applications in electronic and optoelectronic devices<sup>28</sup> and biomedical sensors.<sup>29</sup> In carbon-based field-effect transistors (FETs), HACNT arrays with higher density are often sought,<sup>30</sup>

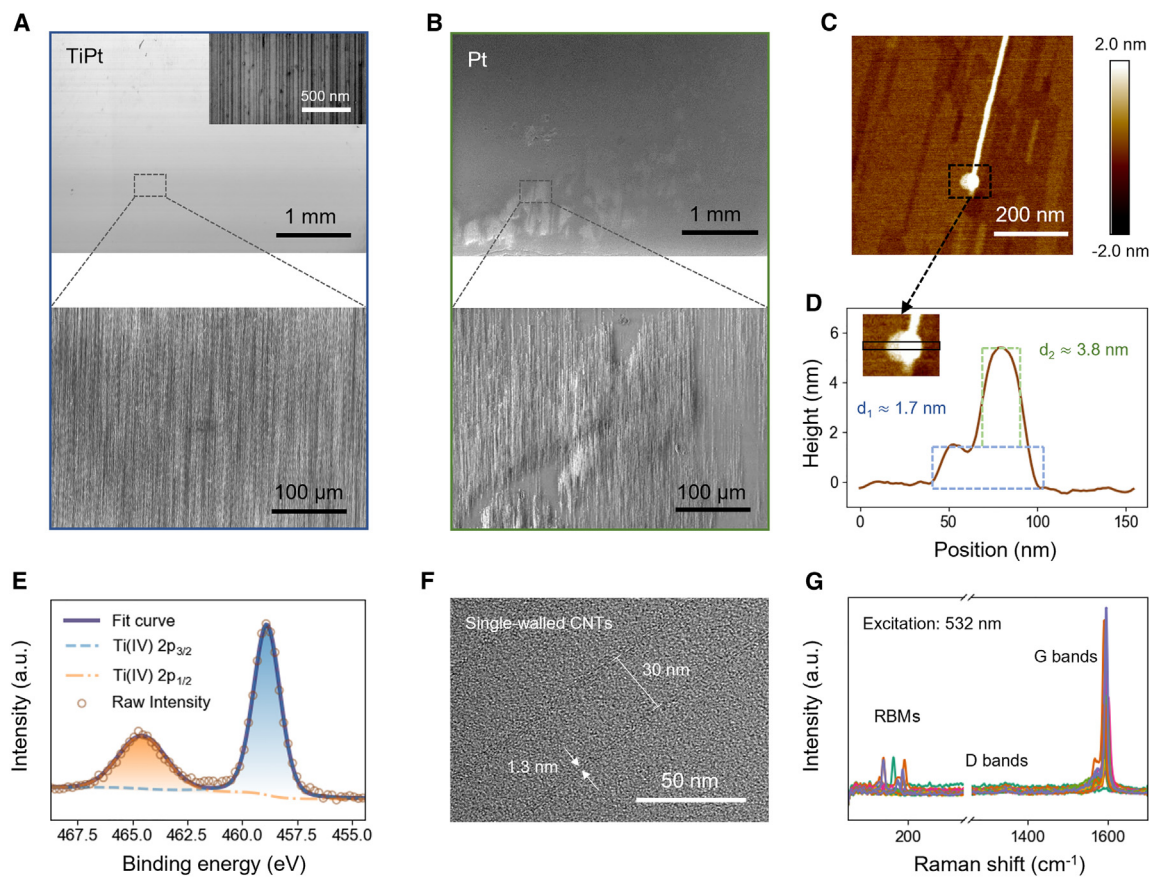


**Figure 3. Characterization of HACNT arrays and catalysts**

- (A) SEM images at different magnifications of HACNT arrays synthesized using TiPt catalysts.
- (B) SEM images at different magnifications of HACNT arrays synthesized using Pt catalysts.
- (C) AFM image of an individual CNT grown with a TiPt catalyst.
- (D) Height profile of the TiPt catalyst corresponding to the AFM image in (C).
- (E) XPS spectrum of the TiPt sample, where fitted Ti peaks indicate the presence of  $\text{Ti}^{4+}$ .
- (F) HRTEM characterization of HACNT arrays with TiPt catalysts.
- (G) Raman spectra of HACNT arrays grown with TiPt catalysts.

while in biomedical sensors and fundamental spectroscopy research, maintaining density within the resolution limits of analytical methods is crucial.<sup>31</sup> Therefore, the ability to customize samples with specific densities is an overwhelming superiority of CVD synthesis and has significant application value.

The key to this challenge lies in establishing the functional relationship between process parameters and sample density. ML methods were employed to handle these multifactorial, nonlinear, and non-monotonic complex relationships. We developed a standardized database using CARCO, comprising over 500 data points including catalysts, growth parameters, and characterization results. Multiple ML models were built to represent the functional relationship between process parameters and predicted sample scores. In essence, these models acted as digital twins of real-world CVD equipment (Figure 4A). In the digital twin, we were able to perform up to one million experiments in 20 min, facilitating a more nuanced exploration of the

CVD growth parameter space. Based on the virtual experiment results, we selected optimal experimental parameters and recommended them for real experimental validation. The outcomes of these real experiments were then added to the database, continuously improving the model in an iterative loop.

The quality of these models directly influences the accuracy of the digital twin experiments. Given that the density of HACNT arrays in the parameter space exhibits a log-normal distribution, we first eliminated samples with a score of 0, then applied a logarithmic transformation to the remaining scores. BO was utilized to find the best parameters for the models, with the RF, gradient boosting regressor (GBR), and XGBoost (XGB) models emerging as winners, achieving  $R^2$  scores of 0.67, 0.65, and 0.64 respectively (Figures 4B, 4C, and S11). Given the inherent randomness in CVD experiments and score assessments, the interpretability of the models for real experimental data was quite satisfying. Predicting the density of HACNT arrays involves both classification (whether growth occurs) and regression (how dense the

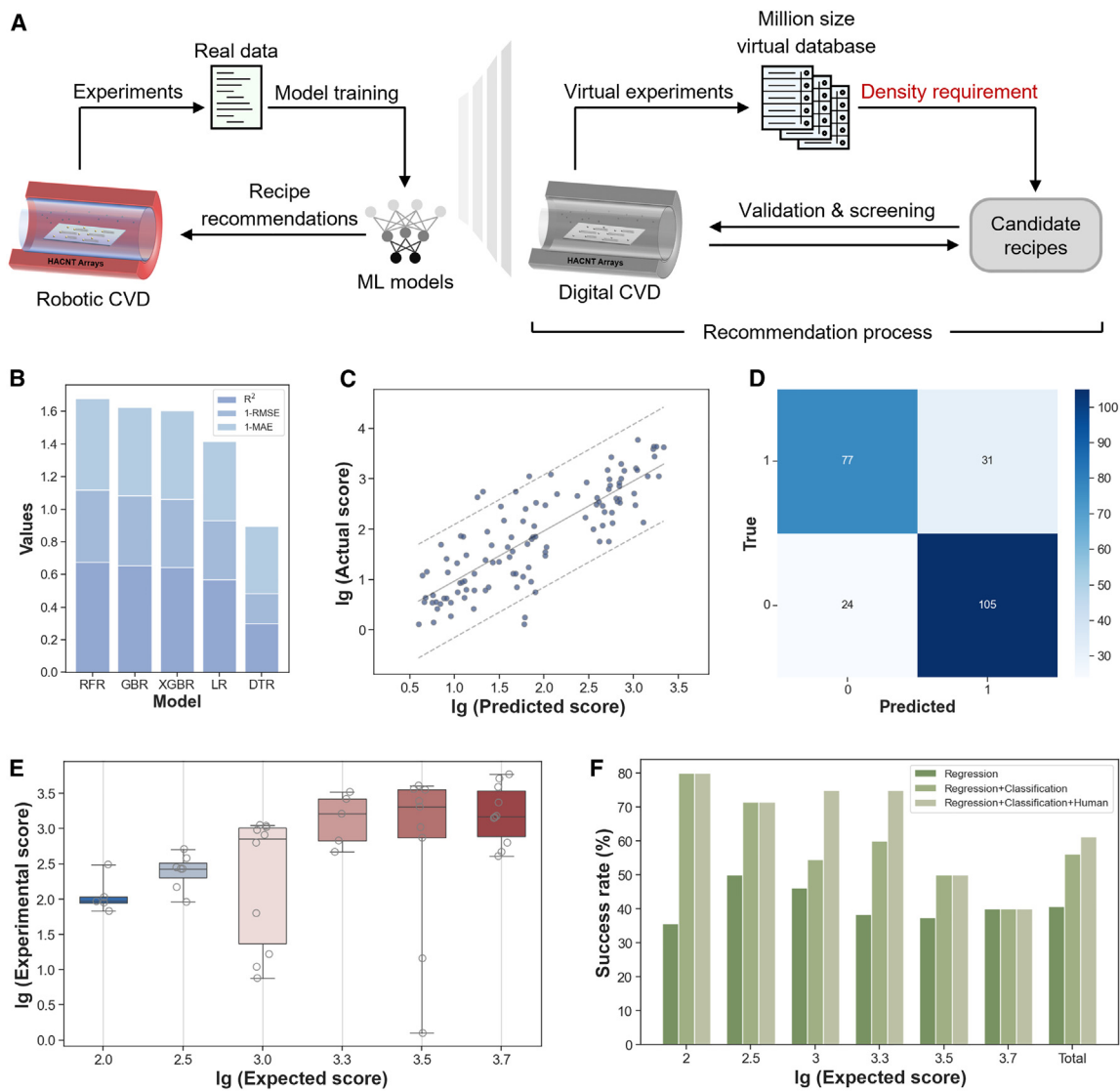


**Figure 4. Density-controllable synthesis**

- (A) Workflow for model establishment and density-controllable synthesis.
- (B) Performance metrics of regression machine learning models.
- (C) The RF model's performance on the test set, with a scatterplot showing the correlation between actual and predicted HACNT density scores.
- (D) Confusion matrix for the classification accuracy of growth occurrence.
- (E) Experimental validation of density-controllable growth, with the x axis representing specified densities and the y axis showing results from real-world experiments.
- (F) Comparative success rates of different approaches: solely regression, regression combined with classification, and incorporating human evaluation.

growth is) problems. Our initial data engineering led to a lack of understanding of the non-growth parameters in regression; thus, we established a separate classification model as a filter to exclude non-growing parameters suggested by the regression models (Figure 4D). Consequently, a **digital twin** comprising four models was constructed, generating a virtual database of experiments on the scale of millions.

Based on this, we developed a workflow for fabricating CNT arrays with specified densities, as depicted in Figure 4A. To achieve a certain density, we simply need to find the closest-

matching process parameters in the virtual database. Using an ensemble-training-like method, we cross-validated the parameters suggested by various models, assigning a credibility score to each set. Finally, the classification model filters out parameters unlikely to result in growth, yielding candidate sets (Table S2). Figures 4E and S12 show the experimental validation of this process. A systematic experimental validation was conducted across a spectrum of densities, ranging from 0.5 to 25 nanotubes per micrometer ( $\lg(\text{score})$ ) ranging from 2 to 3.7, corresponding to scores from 2.0 to 3.7. With a tolerance margin

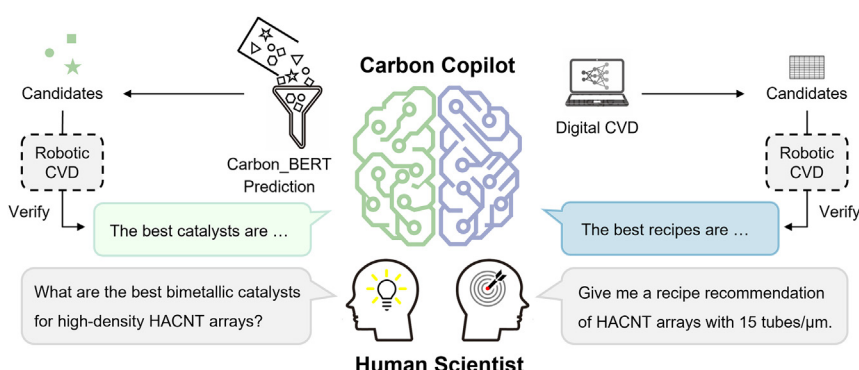


**Figure 5. Interactive workflows with CARCO**

Two workflows, catalyst prediction (left side) and controlled-density growth (right side), demonstrating CARCO's capabilities in innovation and precision manufacturing within CBN synthesis research.

of 10% in Ig (core), the process parameters recommended through the established workflow demonstrated a striking accuracy rate of 56.25% (27/49). This efficacy distinctly surpasses the 39.74% (31/79) accuracy achieved when solely dependent on regression models.

Human brains excel in performing tasks *akin to* a classification model.<sup>32</sup> We had human scientists filter parameters suggested by regression models, achieving an accuracy of 49.15% (29/60), which is lower than that of classification models. Interestingly, when human scientists judged parameters refined through a secondary screening by classification models, the accuracy reached 61.36% (27/45). Human scientists successfully eliminated four sets of parameters that did not meet the specified density targets, reaffirming the *synergy* between human intuition and CARCO suggestions. Figure 4F presents the success rate of parameter recommendations for each density. At lower densities, the candidates provided by regression models contained many that were unviable for growth, likely due to more distinct features, allowing both classification models and human scientists to effectively eliminate poor parameters. At higher specified densities, the parameters suggested by regression models were generally reasonable, making it challenging for classification models and human scientists to identify non-viable parameters. Theoretically, the results mentioned above could be further improved with the expansion of the database. In summary, with the assistance of the CARCO platform, we can achieve precise control that is unattainable with traditional methods, opening up possibilities for the application of HACNT arrays in a broader range of fields.

## DISCUSSION

Our study made valuable contributions to the field of HACNT arrays. By leveraging various modules of CARCO, we have not only achieved catalyst prediction for HACNT array synthesis, corresponding to an innovative challenge, but also accomplished the targeted density growth of HACNT arrays, corresponding to an optimization challenge. Figure 5 illustrates the workflows for accomplishing these two challenges. A noteworthy aspect of our work is the unexpected alignment between Carbon\_BERT's catalyst predictions and the actual experimental results, highlighting the efficacy of embedding methods in the synthesis of CBNs. This alignment led to the innovation of TiPt as a potential dual-

metal catalyst, which exhibits promising attributes compared to traditional iron catalysts for the synthesis of high-density HACNT arrays. Moreover, our platform has enabled the synthesis of HACNT arrays with specified densities, achieving a precision rate of 56.25%, which is "mission impossible" without AI methods. It is worth noting that all the experiments were completed in approximately 1 and a half months. The current efficiency is primarily constrained by the efficiency of nanomaterial characterization.

The vital role of ML in advancing the CBN field has been underscored by this research. A direct advantage observed is the marked increase in experimental throughput and consistency achieved with the robotic CVD, particularly crucial for addressing the complex system challenges inherent in nanomaterial synthesis. The potential of transformer-based language models to inject innovation into nanomaterial research has been validated, possibly due to their ability to facilitate cross-disciplinary creativity, supported by their extensive and diverse training data.<sup>8,13,19</sup> Diverging from other recent "AI for science" publications, this work emphasizes the collaborative synergy between AI and human scientists. This exploration of cooperation is particularly meaningful for nanomaterial research, where characterization and evaluation pose complex challenges. In fact, compared to traditional macroscopic materials, the characterization of nanomaterials presents a higher level of complexity. For example, in our case, for the density of HACNT arrays, it is difficult to obtain high-quality quantitative results with high-throughput and automation-compatible spectroscopic characterization methods, requiring the assistance of human scientists for SEM characterization and measurement. We believe it is important to explore the cooperative pathways between AI agents and human scientists. For the time being at least, CARCO acts as a copilot for human scientists, not a replacement.

Looking toward the future, our study's approach holds immense potential for scalability and adaptability across various nanomaterial systems. The flexibility of our method, anchored in the tailoring of transformer-based language models to specialized domain-specific models, offers a robust framework that can be applied to other domains. The automated CVD platform is naturally suitable for a wide range of nanomaterials like graphene and molybdenum disulfide. Building upon these foundations, the system aims to reshape perspectives in nanomaterial synthesis. The advent of AI technology is set to revolutionize research methodologies. The efficacy of AI in this context is not solely in its standalone capabilities but also significantly in its synergistic collaboration with human scientists. We hope our research can serve as a prototype, demonstrating the profound impact of AI technologies in advancing the nanomaterials field.

## EXPERIMENTAL PROCEDURES

### Construction details of CARCO

GPT and BERT are both transformer-based models but are designed for different purposes. GPT is an autoregressive decoder model, well suited for generating new content. In the CARCO platform, Carbon\_GPT was used for generating high-level suggestions based on prior knowledge. On the other hand, BERT is primarily a bidirectional encoder model, which is excellent for understanding the context and relationships within a given input. In CARCO, it is used to extract structured knowledge from large datasets of scientific texts to evaluate catalyst candidates.

Specifically, to construct the Carbon\_GPT for our CARCO platform, we tailored a GPT specifically for the domain of CBNs, with a particular focus on CNTs. The creation of Carbon\_GPT began with configuring specific instructions and incorporating an extensive knowledge base, selected meticulously to encompass the broad spectrum of research and applications pertaining to CBNs. The primary instructions are as follows.

Carbon GPT, while an expert in carbon materials, focuses predominantly on carbon nanotubes. It offers extensive knowledge from both English and Chinese literature, adapting its responses according to the query's language. The AI's primary functions include: 1) Providing overviews and macro-level guidance on carbon nanotube research, summarizing scientific inquiries, and recommending exploration areas. 2) Detailing preparation methods, applications, and practical advice specifically for carbon nanotubes. 3) Analyzing real-world experimental results related to carbon nanotubes, interpreting data, and offering insights for improvement. While its expertise extends to broader carbon materials, Carbon GPT's core strength and focus remain on carbon nanotubes, ensuring in-depth, tailored responses in this area.

Carbon\_BERT underwent fine-tuning with a comprehensive corpus of literature on carbon materials. On one hand, we selected high-quality literature related to carbon materials and utilized GPT-4 for data cleaning; on the other hand, we used a search engine to filter out texts related to carbon materials and catalysts from the original BERT training data. Together, these formed a knowledge base on carbon materials. In processing the data for fine-tuning, we paid special attention to the structure of the input text. We ensured that distinct lines of text in the dataset were handled as distinct sequences, which is crucial for models designed to understand and generate text based on complex scientific literature. This strategy allowed for a more nuanced and contextually aware learning process, particularly beneficial for the specialized domain of carbon materials.

During the fine-tuning process, we employed the masked language model (MLM) loss function, foundational to BERT's training. By randomly masking tokens in the text and predicting these based on the context of surrounding tokens, we deepened the model's grasp of language structures and domain-specific terminologies. Adjustments to the proportion of masked tokens and the exploration of different learning rates further optimized the model's ability to internalize the intricate vocabulary and concepts central to carbon materials.

To assess the effectiveness of our training approach, we devised 12 specific test questions covering a broad spectrum of topics within the carbon materials and catalyst field. The outcome was a notable improvement in the model's performance, evidenced by the increase of the Spearman correlation coefficient from 0.1 to 0.3.

The robotic CVD system encompasses a CVD central controller, a mini-CVD, a robotic arm, an automated sample holder, and a sample stage. The mini-CVD selected is the Micro-STS1200 from Units Technology. Its compact design and pre-installed optical windows ensure the scalability of the robotic CVD system. Custom sample rods were designed and connected to linear rails, with the sample stage being moved in and out by stepper motors. Optical sensors were installed on both sides for positioning, and a specially designed wedge-shaped furnace opening ensures a good seal under certain pressure conditions. The robotic arm selected is the MG400 from Dobot, used for placing and picking up substrates with a suction nozzle. All modules are centrally controlled by the CVD central controller, which is equipped with a PLC (Panasonic C40ET). It can be operated through a homemade interface or connected to a personal computer (PC) for control.

In constructing the data-driven ML models, we initiated our framework with data engineering. This involved the preprocessing of the dataset where cata-

lyst variables were transformed to one-hot vectors to convert categorical data into a machine-readable format. The synthesis parameters were retained in their original form to maintain the integrity of the experimental conditions. The response variable, "Score" representing the performance of HACNT arrays, was logarithmically transformed to  $\lg(\text{Score})$  to normalize the distribution of the data and stabilize the variance. The dataset was split into training (0.7) and testing (0.3) subsets to ensure the robustness and generalizability of the model. Subsequently, RFR, GBR, XGBR, logistic regression (LR), and decision tree regression (DTR) were developed, respectively. We employed BO as a strategic approach to refine the hyperparameters of the model. This process began by defining a range for each hyperparameter, which guided the optimization algorithm. The Bayesian optimizer was then initialized to explore the hyperparameter space, balancing the trade-off between exploration of new parameters and exploitation of ones known to be effective. The objective function to maximize was the cross-validated performance of the model on the training set. The output of the BO provided a set of best hyperparameters, which were used to train the final ML models. The performance of the models was evaluated using the  $R^2$  score, mean absolute error (MAE), and root-mean-square error (RMSE) on the testing set. These metrics provided insights into the accuracy and reliability of the model's predictions (Figure S13; Note S4).

In addition to regression analysis, we also implemented a binary classification to distinguish between growth and non-growth samples. This was achieved by creating binary labels from the score with a defined threshold. A pipeline was established to streamline the process of predicting the likelihood of growth occurrence. The process concluded with an evaluation of the model's performance, ensuring the accuracy and efficacy of the predictions (Figure S14).

### Catalyst screening

In the initial phase of catalyst screening, we established a comprehensive list that consisted of a series of questions along with a list of potential candidate catalysts. For the processing of our textual data, the BertTokenizer from the transformers library was employed to convert the text into a format comprehensible by the model. The BertModel, a PyTorch implementation of BERT, was utilized to operationalize the pre-trained Carbon\_BERT model. This setup facilitated the conversion of all listed words into embeddings, effectively capturing the contextual relationships inherent in the language model's training data. The embeddings for each word in the list were generated by passing the text through the tokenizer and subsequently through the model, focusing on extracting the last hidden state of the [CLS] token representation, where [CLS] stands for Classification Token, serving as an aggregate embedding for the input sequence.

Upon obtaining the embeddings, the cosine similarity between the question embedding and each of the candidate catalyst embeddings was computed. This metric evaluates the cosine of the angle between the vectors in the embedding space, generating a similarity matrix. The similarity scores specific to the predefined query regarding high-density HACNT array synthesis were extracted, and the candidate catalysts were ranked according to their cosine similarity to the query. This ranking indicated the likelihood of each catalyst's efficacy in enhancing the density of HACNT arrays, thereby guiding the selection process toward the most promising candidates for further experimental validation.

### Growth and characterization of HACNT arrays

We utilized a-plane sapphire substrates (single-side polished, miscut angle  $< 0.5^\circ$ , surface roughness  $< 0.5 \text{ nm}$ ) for the preparation of HACNT arrays, which were acquired from Hefei Kejing Materials Technology, China. The initial stage involved loading the catalysts onto the substrates using ion implantation technology conducted at room temperature. This implanter (FAD-MEVVA) is equipped with a uniform beam spot exceeding 8 inches in diameter,<sup>33</sup> a specification verified using Gafchromic EBT3 self-developing dosimetry film.<sup>34</sup> Such uniformity enables the concurrent implantation of catalysts into five 3 inch sapphire wafers, with each wafer segmented into roughly 160 samples measuring  $4 \times 6 \text{ cm}^2$ . As a result, each implantation cycle can consistently deposit catalysts on approximately 800 samples. The ion fluence was controlled within a range from  $1\text{E}13$  to  $1\text{E}16 \text{ ions/cm}^2$ , and the ion energies were adjusted between 5 and 20 keV. We employed a range of elements including Fe, Co, Ni,

Cu, Ti, Pt, and Ru. The physical phenomena of ion implantation were examined using The Stopping and Range of Ions in Matter (SRIM) software suite. Specifically, the Monte Carlo-based Transport of Ions in Matter (TRIM) simulation was implemented to probe the interactions between energetic ions and the sapphire substrates.<sup>35</sup>

After the ion implantation, the samples were sequentially ultrasonically cleaned in deionized water, acetone, and ethanol. An annealing process at 1,100°C in an air atmosphere for 5 h was then conducted. This step was crucial in **mending** the radiation-induced damages to the substrate surface from the implantation.

The growth process was fully automated by the robotic CVD system. Substrates were **conveyed into** the mini-CVD by the robotic arm and automated sample holder. Upon the initiation of the growth cycle, the system was programmed to reach the predetermined temperature in 15 min. Once the target temperature was achieved, the system sequentially executed the reduction and growth phases. Following the growth cycle, the temperature was rapidly reduced by water cooling, taking approximately 7 min for the system to reach 150°C. At this point, the samples were automatically retrieved by the sample holder and robotic arm, and the system proceeded to the next set of growth tasks.

The parameter space for the synthesis was defined with specific ranges to optimize the conditions for HACNT array growth. The parameters were set as follows: temperature, ranging from 800 to 1,000°C; reduction time, ranging from 1 to 1,000 s; growth time, ranging from 1 to 1,000 s; argon flow, ranging from 50 to 500 sccm; hydrogen flow, ranging from 15 to 500 sccm; and ethanol flow, **bubbling** by argon flow, ranging from 1.7 to 118.3 sccm.

A typical experimental workflow and timeline overview is shown in [Note S5](#).

#### Performance evaluation of HACNT arrays

We performed general characterization of HACNT arrays, including SEM, Raman, XPS, HRTEM, and AFM analyses ([Figures 3 and S15](#)). SEM images were obtained on a Hitachi S4800 SEM operated at 1.0 and 10 kV. Raman spectra of HACNT arrays with line mapping conducted with a step of 5 μm and a laser beam spot of ~1 μm were collected from Jovin Yvon-Horiba LabRam systems with 532 nm excitation. XPS spectra were obtained on AXIS Supra, HRTEM spectra were obtained on JEM-F200, and AFM images were obtained using a Dimension Icon microscope (Bruker).

The score of HACNT arrays is composed of two aspects: density and orientation. Density is computed using a Python-based recognition program that was custom developed for this purpose, while the orientation is subjectively evaluated to obtain a penalty factor. Scores for each sample are then determined through a standardized computational method ([Figure S3](#)).

#### RESOURCE AVAILABILITY

##### Lead contact

Requests for further information and resources should be directed to and will be fulfilled by the lead contact, Jin Zhang ([jinzhang@pku.edu.cn](mailto:jinzhang@pku.edu.cn)).

##### Materials availability

This study did not generate new unique reagents.

##### Data and code availability

- All data supporting the findings of this study are included in the manuscript and its [supplemental information](#) or are available from the corresponding authors upon reasonable request.
- All the code/model for CARCO were openly released on Zenodo (<https://doi.org/10.5281/zenodo.13922366>).

#### ACKNOWLEDGMENTS

This work was financially supported by the Ministry of Science and Technology (China) (2022YFA1203302, 2022YFA1203304, and 2018YFA0703502), the National Natural Science Foundation of China (grant nos. 52021006, 52102032, and 52272033), the Strategic Priority Research Program of CAS (XDB36030100), the Beijing National Laboratory for Molecular Sciences

(BNLMS-CXTD-202001), and the Shenzhen Science and Technology Innovation Commission (KQTD20221101115627004).

#### AUTHOR CONTRIBUTIONS

Y.L. and S.W. prepared the samples and performed the experiments of synthesizing and characterizing HACNT arrays, assisted by Y.Z., Y. Xie, and Y. Xu. Y.L. designed and constructed the CARCO platform. Z.W. conducted the fine-tuning of language models, supervised by Y.Y., Y.L., L.Q., and S.W. wrote and revised the manuscript with input from all authors. J.Z., L.Q., Z.L., and Z.Z. supervised the overall projects. All authors contributed to the discussion and completion of this manuscript.

#### DECLARATION OF INTERESTS

The authors declare no competing interests.

#### SUPPLEMENTAL INFORMATION

Supplemental information can be found online at <https://doi.org/10.1016/j.matt.2024.11.007>.

Received: June 22, 2024

Revised: October 19, 2024

Accepted: November 7, 2024

Published: December 2, 2024

#### REFERENCES

1. Kolahdouz, M., Xu, B., Nasiri, A.F., Fathollahzadeh, M., Manian, M., Aghababa, H., Wu, Y., and Radamson, H.H. (2022). Carbon-Related Materials: Graphene and Carbon Nanotubes in Semiconductor Applications and Design. *Micromachines* 13, 1257. <https://doi.org/10.3390/mi13081257>.
2. Qian, L., Xie, Y., Zou, M., and Zhang, J. (2021). Building a Bridge for Carbon Nanotubes from Nanoscale Structure to Macroscopic Application. *J. Am. Chem. Soc.* 143, 18805–18819. <https://doi.org/10.1021/jacs.1c0554>.
3. Hills, G., Lau, C., Wright, A., Fuller, S., Bishop, M.D., Srimani, T., Kanhaiya, P., Ho, R., Amer, A., Stein, Y., et al. (2019). Modern microprocessor built from complementary carbon nanotube transistors. *Nature* 572, 595–602. <https://doi.org/10.1038/s41586-019-1493-8>.
4. Luo, J., Wen, Y., Jia, X., Lei, X., Gao, Z., Jian, M., Xiao, Z., Li, L., Zhang, J., Li, T., et al. (2023). Fabricating strong and tough aramid fibers by small addition of carbon nanotubes. *Nat. Commun.* 14, 3019. <https://doi.org/10.1038/s41467-023-38701-4>.
5. Yu, D., Goh, K., Wang, H., Wei, L., Jiang, W., Zhang, Q., Dai, L., and Chen, Y. (2014). Scalable synthesis of hierarchically structured carbon nanotube–graphene fibres for capacitive energy storage. *Nat. Nanotechnol.* 9, 555–562. <https://doi.org/10.1038/nnano.2014.93>.
6. Taylor, C.J., Pomberger, A., Felton, K.C., Grainger, R., Barecka, M., Chamberlain, T.W., Bourne, R.A., Johnson, C.N., and Lapkin, A.A. (2023). A Brief Introduction to Chemical Reaction Optimization. *Chem. Rev.* 123, 3089–3126. <https://doi.org/10.1021/acs.chemrev.2c00798>.
7. Jordan, M.I., and Mitchell, T.M. (2015). Machine learning: Trends, perspectives, and prospects. *Science* 349, 255–260. <https://doi.org/10.1126/science.aaa8415>.
8. Szymanski, N.J., Rendy, B., Fei, Y., Kumar, R.E., He, T., Milsted, D., McDermott, M.J., Gallant, M., Cubuk, E.D., Merchant, A., et al. (2023). An autonomous laboratory for the accelerated synthesis of novel materials. *Nature* 624, 86–91. <https://doi.org/10.1038/s41586-023-06734-w>.
9. Pei, Z., Yin, J., Liaw, P.K., and Raabe, D. (2023). Toward the design of ultrahigh-entropy alloys via mining six million texts. *Nat. Commun.* 14, 54. <https://doi.org/10.1038/s41467-022-35766-5>.

10. Tao, H., Wu, T., Aldeghi, M., Wu, T.C., Aspuru-Guzik, A., and Kumacheva, E. (2021). Nanoparticle synthesis assisted by machine learning. *Nat. Rev. Mater.* 6, 701–716. <https://doi.org/10.1038/s41578-021-00337-5>.
11. Salley, D., Keenan, G., Grizou, J., Sharma, A., Martín, S., and Cronin, L. (2020). A nanomaterials discovery robot for the Darwinian evolution of shape programmable gold nanoparticles. *Nat. Commun.* 11, 2771. <https://doi.org/10.1038/s41467-020-16501-4>.
12. Tao, H., Wu, T., Kheiri, S., Aldeghi, M., Aspuru-Guzik, A., and Kumacheva, E. (2021). Self-Driving Platform for Metal Nanoparticle Synthesis: Combining Microfluidics and Machine Learning. *Adv. Funct. Mater.* 31, 2106725. <https://doi.org/10.1002/adfm.202106725>.
13. Boiko, D.A., MacKnight, R., Kline, B., and Gomes, G. (2023). Autonomous chemical research with large language models. *Nature* 624, 570–578. <https://doi.org/10.1038/s41586-023-06792-0>.
14. Franklin, A.D. (2015). Nanomaterials in transistors: From high-performance to thin-film applications. *Science* 349, aab2750. <https://doi.org/10.1126/science.aab2750>.
15. Vaswani, A., Shazeer, N., Parmar, N., Uszkoreit, J., Jones, L., Gomez, A.N., Kaiser, L., and Polosukhin, I. (2017). Attention is All you Need. Preprint at arXiv. <https://doi.org/10.48550/arXiv.1706.03762>.
16. OpenAI; Achiam, J., Adler, S., Agarwal, S., Ahmad, L., Akkaya, I., Aleman, F.L., Almeida, D., Altenschmidt, J., Altman, S., et al. (2024). GPT-4 Technical Report. Preprint at arXiv. <https://doi.org/10.48550/arXiv.2303.08774>.
17. Devlin, J., Chang, M.-W., Lee, K., and Toutanova, K. (2019). BERT: Pre-training of Deep Bidirectional Transformers for Language Understanding. Preprint at arXiv. <https://doi.org/10.48550/arXiv.1810.04805>.
18. Ganesh, P., Chen, Y., Lou, X., Khan, M.A., Yang, Y., Sajjad, H., Nakov, P., Chen, D., and Winslett, M. (2021). Compressing Large-Scale Transformer-Based Models: A Case Study on BERT. *Trans. Assoc. Comput. Linguist.* 9, 1061–1080. [https://doi.org/10.1162/tacl\\_a\\_00413](https://doi.org/10.1162/tacl_a_00413).
19. Slattery, A., Wen, Z., Tenblad, P., Sanjosé-Orduna, J., Pintossi, D., Den Hartog, T., and Noé, T. (2024). Automated self-optimization, intensification, and scale-up of photocatalysis in flow. *Science* 383, ead1817. <https://doi.org/10.1126/science.adj1817>.
20. He, M., Zhang, S., and Zhang, J. (2020). Horizontal Single-Walled Carbon Nanotube Arrays: Controlled Synthesis, Characterizations, and Applications. *Chem. Rev.* 120, 12592–12684. <https://doi.org/10.1021/acs.chemrev.0c00395>.
21. Zhang, S., Kang, L., Wang, X., Tong, L., Yang, L., Wang, Z., Qi, K., Deng, S., Li, Q., Bai, X., et al. (2017). Arrays of horizontal carbon nanotubes of controlled chirality grown using designed catalysts. *Nature* 543, 234–238. <https://doi.org/10.1038/nature21051>.
22. Ding, F., Bolton, K., and Rosén, A. (2004). Nucleation and Growth of Single-Walled Carbon Nanotubes: A Molecular Dynamics Study. *J. Phys. Chem. B* 108, 17369–17377. <https://doi.org/10.1021/jp046645t>.
23. Tshitoyan, V., Daggelen, J., Weston, L., Dunn, A., Rong, Z., Kononova, O., Persson, K.A., Ceder, G., and Jain, A. (2019). Unsupervised word embeddings capture latent knowledge from materials science literature. *Nature* 571, 95–98. <https://doi.org/10.1038/s41586-019-1335-8>.
24. He, T., Huo, H., Bartel, C.J., Wang, Z., Cruse, K., and Ceder, G. (2023). Precursor recommendation for inorganic synthesis by machine learning materials similarity from scientific literature. *Sci. Adv.* 9, eadg8180. <https://doi.org/10.1126/sciadv.adg8180>.
25. Yuan, D., Ding, L., Chu, H., Feng, Y., McNicholas, T.P., and Liu, J. (2008). Horizontally Aligned Single-Walled Carbon Nanotube on Quartz from a Large Variety of Metal Catalysts. *Nano Lett.* 8, 2576–2579. <https://doi.org/10.1021/nl801007r>.
26. Wrobel, S. (2010). An Efficient Explanation of Individual Classifications using Game Theory. *J. Mach. Learn. Res.* 11, 1–18. <https://dl.acm.org/doi/10.5555/1756006.1756007>.
27. Tian, Z., Da, Y., Wang, M., Dou, X., Cui, X., Chen, J., Jiang, R., Xi, S., Cui, B., Luo, Y., et al. (2023). Selective photoelectrochemical oxidation of glucose to glucaric acid by single atom Pt decorated defective TiO<sub>2</sub>. *Nat. Commun.* 14, 142. <https://doi.org/10.1038/s41467-023-35875-9>.
28. Avouris, P., Freitag, M., and Perebeinos, V. (2008). Carbon-nanotube photonics and optoelectronics. *Nat. Photonics* 2, 341–350. <https://doi.org/10.1038/nphoton.2008.94>.
29. Kruss, S., Hilmer, A.J., Zhang, J., Reuel, N.F., Mu, B., and Strano, M.S. (2013). Carbon nanotubes as optical biomedical sensors. *Adv. Drug Deliv. Rev.* 65, 1933–1950. <https://doi.org/10.1016/j.addr.2013.07.015>.
30. Xie, Y., Li, Y., Zhao, Z., and Zhang, J. (2023). Pave the way to the batch production of SWNT arrays for carbon-based electronic devices. *Nano Res.* 16, 12516–12530. <https://doi.org/10.1007/s12274-023-6173-1>.
31. Hueso, L.E., Pruneda, J.M., Ferrari, V., Burnell, G., Valdés-Herrera, J.P., Simons, B.D., Littlewood, P.B., Artacho, E., Fert, A., and Mathur, N.D. (2007). Transformation of spin information into large electrical signals using carbon nanotubes. *Nature* 445, 410–413. <https://doi.org/10.1038/nature05507>.
32. Grinband, J., Hirsch, J., and Ferrera, V.P. (2006). A Neural Representation of Categorization Uncertainty in the Human Brain. *Neuron* 49, 757–763. <https://doi.org/10.1016/j.neuron.2006.01.032>.
33. Zhang, T., Wang, X., Liang, H., Zhang, H., Zhou, G., Sun, G., Zhao, W., and Xue, J. (1996). Behaviour of MEVVA metal ion implantation for surface modification of materials. *Surf. Coatings. Technol.* 83, 280–283. [https://doi.org/10.1016/0257-8972\(96\)02855-1](https://doi.org/10.1016/0257-8972(96)02855-1).
34. Sharma, M., Singh, R., Dutt, S., Tomar, P., Trivedi, G., and Robert, N. (2021). Effect of absorbed dose on post-irradiation coloration and interpretation of polymerization reaction in the Gafchromic EBT3 film. *Radiat. Phys. Chem.* 187, 109569. <https://doi.org/10.1016/j.radphyschem.2021.109569>.
35. Ziegler, J.F., Ziegler, M.D., and Biersack, J.P. (2010). SRIM – The stopping and range of ions in matter (2010). *Nucl. Instrum. Methods Phys. Res. Sect. B Beam Interact. Mater. Atoms* 268, 1818–1823. <https://doi.org/10.1016/j.nimb.2010.02.091>.